# Double Photodetachment of $F^-\cdot H_2O$: Experimental and Theoretical Studies of $[F\cdot H_2O]^+$

*Abhishek Shahi,* [‡, a] *Laura McCaslin,* [‡, b] *Yishai Albeck,* [‡, a] *Robert E. Continetti,* [c] *R. Benny Gerber* [b, d] *and Daniel Strasser* [*, a]

[a] Institute of Chemistry, The Hebrew University of Jerusalem, Jerusalem, 91904, Israel

[b] Fritz Haber Center for Molecular Dynamics, Institute of Chemistry, The Hebrew University of Jerusalem, Jerusalem, 91904, Israel

[c] Department of Chemistry and Biochemistry, University of California San Diego, La Jolla, CA, 92093-0340, USA.

[d] Department of Chemistry, University of California, Irvine, California 92697, USA

**TOC GRAPHIC:**

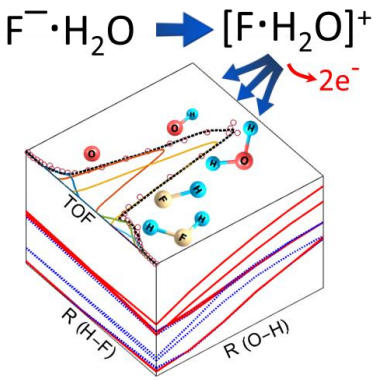

Double photodetachment of the cluster $F^-\cdot H_2O$ in a strong laser field is explored in a combined experimental-theoretical study. Products are observed experimentally by coincidence photofragment imaging following double ionization by intense laser pulses. Theoretically, equation of motion coupled cluster calculations (EOM-CC), suitable for modeling strong correlation effects in the electronic wavefunction, shed light on the Franck-Condon region and *ab initio* molecular dynamics (AIMD) simulations also performed using EOM-CC methods reveal the fragmentation dynamics in time on the lowest lying singlet and triplet states of $[F\cdot H_2O]^+$. The simulations show the formation of $H_2O^+$ + F, which is the predominant experimentally observed product channel. Suggestions are proposed for the formation mechanisms of the minor products, e.g. the very interesting $H_2F^+$, which involves significant geometrical rearrangement. Analysis of the results suggests interesting future directions for the exploration of photodetachment of anionic clusters in an intense laser field.

**KEYWORDS**: Photodissociation, Photodetachment, Fast beam experiment, 3D imaging, Intense field, Ab initio Molecular Dynamics.

**Note:** ‡ Authors contribute equally.

* Author Information: strasser@huji.ac.il

Photodetachment and photoionization are fundamental processes following the interaction of light with isolated atomic, molecular and cluster systems. When these processes occur as a result of intense femtosecond laser pulses, they exhibit a broad range of non-linear phenomena including high harmonic generation and enhanced double ionization.[1–5] Both processes are successfully described by a tunnel-ionized electron, driven by a strong laser field, recolliding with its parent system.[3] This semiclassical picture dominates intense laser pulse interactions with neutral systems, offering an intuitive view of attosecond science.[6] Furthermore, the excess energy deposited by the intense laser pulse can result in surprising photochemistry.[7,8]

Anionic systems can be expected to exhibit new and less understood mechanisms of intense field interaction with matter.[9–13] Sequential photodetachment of two electrons from an isolated anion by two separate laser pulses has been used to study dynamics on intermediate neutral species.[14,15] In contrast, intense-laser experiments performed on atomic, molecular and cluster anions have revealed efficient non-sequential detachment of multiple electrons,[13,16,17] which cannot be described by the recollision dynamics that successfully model the analogous double-ionization of neutral species. These molecular and cluster systems exhibit significant fragmentation of the cationic products of double detachment. Even for systems with a stable cation, intense-laser double-detachment led to dissociative ionization.[18,19] For tightly bound molecular anionic systems such as $F_2^-$ and $SF_6^-$, the surprisingly high kinetic energy release (KER) measured between the fragments was attributed to excitation to high lying states composed of a strongly repulsive dication core and a Rydberg electron.[18,19] Excitation away from equilibrium as a result of strong laser pulses leads one to imagine substantial structural rearrangement, leading to

formation of new chemical bonds. $F^-\cdot(NF_3)_n$ clusters, bound by relatively weak electrostatic interaction, were shown to exhibit intense laser double detachment without significant geometrical rearrangement.[16] Nevertheless, it is appealing to study multiple detachment of hydrogen-bonded $F^-\cdot(H_2O)_n$ clusters,[20] because new bond formation is more likely for systems with stronger non-covalent interactions. Furthermore, roaming hydrogen dynamics can be expected to enrich the range of possible structural rearrangement and formation of new bonds.[21–25]

Reactivity of such water-solvated halides has been extensively studied.[20,26] Thermal reactions of $F^+$ and $H_2O$ in bulk water were shown to yield the $HF^+$ reactive product along with the dominant charge transfer product $H_2O^+$ and its fragments.[27,28] In the simplest anionic $F^-\cdot H_2O$ cluster the hydrogen bond is particularly strong, with a 1.35 Å F-H bond length.[29] Photodetachment launches a wavepacket near the transition state of the neutral $F + H_2O \rightarrow HF + OH$ reaction.[30–34] Photoelectron-photofragment coincidence measurements established the role of several electronic states participating in dissociation to produce either $F + H_2O$ or hydrogen abstraction to form HF + OH.[32,35] In this work we present a joint experimental and theoretical exploration of intense laser double-detachment of $F^-\cdot H_2O$, generating cationic species including $H_2F^+$: a product requiring significant structural rearrangement from its parent anion geometry, which was not reported on the neutral reactive surface.

Our fast beam fragment imaging spectrometer allows simultaneous detection of possible anionic, cationic, as well as neutral fragments resulting from interaction of ultrafast intense laser pulses with mass selected anion systems.[36] Three-dimensional coincidence imaging of laser-anion interaction products allows us to disentangle the different fragmentation channels.[18,19] Figure 1 shows coincidence map analysis of

correlated fragments of the $F^-\cdot H_2O$ complex allowing assignment of the observed dissociation events based on each fragment's time of flight (TOF). Contour "a" indicates two correlated fragments corresponding to two neutral dissociative detachment products. Contour "b" marks events of correlated neutral and cationic fragments, corresponding to dissociative ionization following double detachment. Contours "c" and "d" indicate Coulomb explosion channels, where the latter includes the $O^{2+}$ dication. We did not detect any significant yields of anionic fragments. Furthermore, within experimental sensitivity, intense-field double-detachment of the $F^-\cdot H_2O$ did not produce the stable $[F\cdot H_2O]^+$ parent cation.

Figure 1 inset shows the dependence of different channel yields on laser peak intensity. The measurement is performed by systematic displacement of the laser focal point from the anion target, referred to as "z-scan" analysis.[37] As can be expected, ionization channels associated with greater number of detached electrons exhibit higher saturation intensities, as indicated by maximal yields reached at higher laser intensities and lower z-displacements from the laser focal point. Dissociative detachment yields decrease monotonically with diminishing z-displacement, indicating saturation below $10^{14}$ W/cm$^2$. On the other extreme, the $O^{2+}$ dication channel does not saturate and reaches its maximal yield near the focal point corresponding to $3\cdot10^{15}$ W/cm$^2$. However, Coulomb explosion involving only singly ionized products exhibits maximal yield at $I_{max}\sim8\pm4\cdot10^{14}$ W/cm$^2$. Double detachment followed by dissociative ionization saturates at lower intensities with a maximum at $I_{max}\sim 2\pm0.5\cdot10^{14}$ W/cm$^2$. The corresponding saturation intensities, which for Gaussian laser pulses are related to $I_{max}$ by a geometric factor of ~3,[37] are similar to those previously reported for enhanced non-sequential double detachment of other molecular and cluster anions.[16–19]

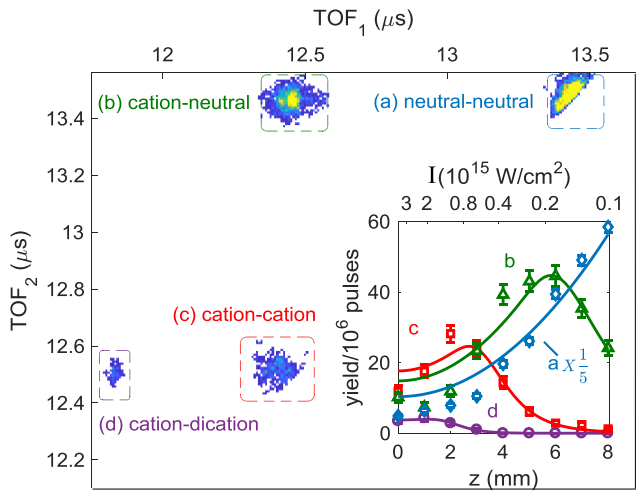


Figure 1: Coincidence plot of (a) single-detachment, (b) double-detachment and (c-d) Coulomb explosion channels. Inset shows yields as a function of laser peak intensity and corresponding displacement, z, from the laser focal point.

Figure 2 shows the measured cation TOF distribution, detected in coincidence with a neutral product. The kinetic energy released upon dissociation leads to recoil along the TOF axis, resulting in overlap of neighboring cation masses, making individual event assignment unfeasible. Nevertheless, as shown in Figure 2, it is possible to deconvolute the contributions of different channels by fitting the measured TOF distribution with simulated dissociative ionization distributions.[36] Independent proton and neutral hydrogen products could not be detected in these experiments due to their low lab-frame momenta. In contrast to the reactive HF + OH products observed for single photodetachment, the major channel of dissociative ionization is $H_2O^+$ + F that requires no structural rearrangement beyond H-F bond dissociation. The $OH^+$ and $O^+$ fragments of $H_2O$ are also detected. Interestingly, within the experimental error limit, we did not observe the expected $F^+$ product throughout the explored intensity range. Furthermore, contributions from the more surprising and interesting products, $HF^+$ and $H_2F^+$, had to be included to successfully fit the experimentally measured data. The $HF^+$ product can in principle

be formed via proton transfer from the parent $H_2O$ moiety to the fluorine. However, formation of the $H_2F^+$ must involve more significant hydrogen motion dynamics on the cation potential surface. This mechanism is possibly due to rearrangement from the FC geometry towards the $[HFH\text{-}O]^+$ local minimum calculated by Luna *et.al.* on the cationic potential surface.[28] Figure 2 inset shows the cation branching ratio as a function of laser peak intensity for the dominant $H_2O^+$ cation, the collective yield of $OH^+$ and $O^+$ fragments, and the sum of the reactive channels forming $HF^+$ or $H_2F^+$. While the measured branching ratios remain nearly constant throughout the 0.1-3 $PW/cm^2$ peak intensity range, the linear fit helps guide the eye to reveal a systematic increase in $OH^+$ and $O^+$ yields with increasing peak intensity, at the expense of the water cation, reflecting increased fragmentation of the $H_2O$ moiety at high peak intensities.

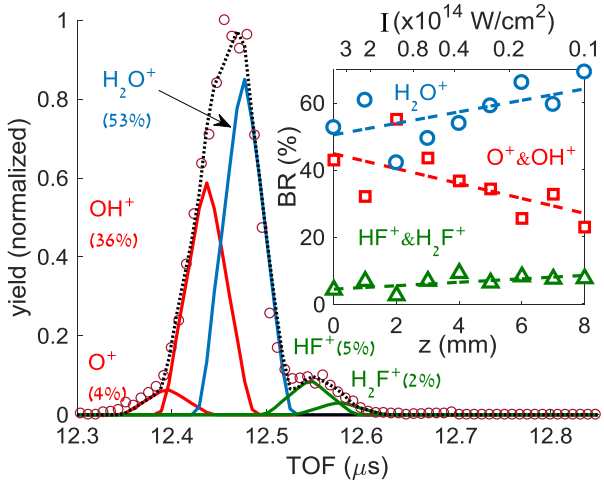


**Figure 2:** TOF spectrum of double detachment products: cations recorded in coincidence with a neutral product. Solid lines show the simulated yields of different channels and their fitted intensities that reconstruct the experimental data points (open circles) with the dotted line. The figure inset shows the branching ratios as a function of peak intensity (or z-position).

From a theoretical standpoint, there are numerous difficulties in the exact description of $F^{-}\cdot H_2O$ double photodetachment by an intense laser field. Our goal is therefore to determine if the experimentally observed products can be formed on the cationic $[F\cdot H_2O]^+$ complex and its excited states. This requires a detailed understanding of the Franck-Condon (FC) region and its connection to fragmentation pathways. Furthermore, possible multi-dimensional paths towards the surprising $H_2F^+$ product will be explored by high level AIMD simulations.

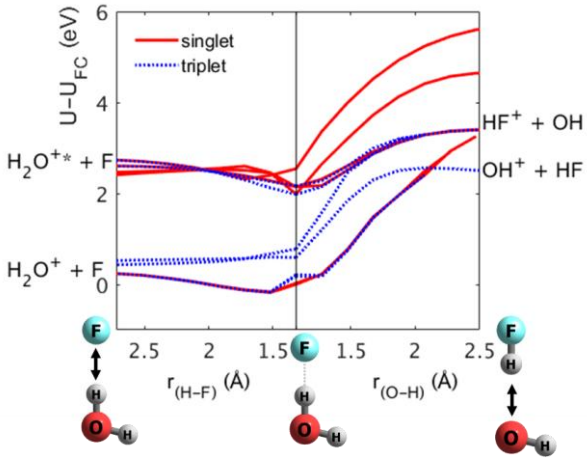


**Figure 3**: Potential energy curves calculated at the EOM-CCSD(dT)/cc-pVTZ level of theory along both the H-F and O-H bond length coordinates are presented, extending from the FC geometry.

Figure 3 shows the potentials of the $[F\cdot H_2O]^+$ system along two reaction coordinates, calculated relative to $U_{FC}$, the cation ground state potential at the FC geometry. Both plots extend from the center, corresponding to the FC geometry. On the left-hand side, the energies are shown along the H-F distance coordinate corresponding to separation of $H_2O$ and F fragments, keeping all other coordinates fixed and thus unrelaxed. The lowest-lying curves are of the nearly degenerate singlet and triplet ground states. These lowest-lying curves asymptotically converge just above 0 eV to form $H_2O^+$ + F products, indicating that this is a probable

dissociation channel, as the unrelaxed separated fragments in the plots are expected to be higher in energy than their relaxed counterparts. Indeed, as summarized in table 1, the relaxed $H_2O^+ + F$ product channel energy lies at -0.34eV below $U_{FC}$, the ground state energy at the FC geometry. This is in qualitative agreement with the ~0.2 ± 0.13 eV KER used to successfully simulate the measured cation-neutral coincidence spectra. The analogous infinitely separated relaxed $H_2O + F^+$ product channel is calculated to be much higher in energy, at +4.41eV above $U_{FC}$, in agreement with the experimental finding of negligible $F^+$ yield. On the right side of figure 3, the energies are shown along the coordinate corresponding to separation of OH and HF fragments along the O-H distance, keeping all other coordinates fixed. As opposed to the neutral potential surface,[38,39] all the cation curves rise rapidly with the lowest curve. However, the energies of the relaxed product channels, which are summarized in table 1, demonstrate that concerted O-H separation and relaxation of the remaining HF and OH bonds make the $OH^+ + HF$ channel energetically favored at -0.61 eV below $U_{FC}$. When comparing formation of $OH^+ + HF$ vs. $HF^+ + OH$, the relaxed dissociation limits of -0.61 eV vs. 2.44 eV agree with the experimental contributions of ~36% and ~5%, respectively. Table 1 shows also the relaxed energetic limits of channels that require significant structural rearrangement. As neutral $H_2F$ is unstable relative to its fragments, the relaxed limit corresponding to the $O^+$ cation is a three-body fragmentation channel, requiring excitation of over +4.42 eV above $U_{FC}$. In contrast, the surprising $H_2F^+$ product is in fact the most energetically favorable channel at -0.74eV below the $U_{FC}$ potential.

**Table 1**: Relative energies of the relaxed product states of $[F{\cdot}H_2O]^+$ at CCSD(T)/cc-PVTZ level of theory.

| Products | $U - U_{FC}$ (eV) |
|---|---|
| $H_2F^+ + O$ | -0.74 |
| $OH^+ + HF$ | -0.61 |
| $H_2O^+ + F$ | -0.34 |
| $HF^+ + OH$ | 2.44 |
| $F^+ + H_2O$ | 4.41 |
| $O^+ + H + HF$ | 4.42 |

Although the relaxed asymptotic energies and energy curves along candidate dissociation coordinates provide valuable insights about the observed product branching ratios, it is imperative to evaluate the role of dynamics. The experimental branching ratios favor the $H_2O^+$ cation, formed without structural rearrangement, over the energetically favorable $OH^+$ and $H_2F^+$, which do require structural rearrangement and formation of new bonds. Roaming hydrogen dynamics are ubiquitously found in dissociative photoionization, resulting in structural rearrangement.[25] Here, $H_2F^+$ formation requires an intricate migration of both hydrogen atoms within the ionized cluster, from their parent water moiety to the F atom. To further explore possible geometrical rearrangement of the system, AIMD simulations were performed on the ground state singlet and triplet cation surfaces using equation of motion coupled cluster theory with single and double excitations (EOM-CCSD).[40–43] EOM-CCSD is a highly correlated electronic structure method suitable for the dense electronic states in the cation complex.[44] Only one trajectory, run on the singlet surface, did not result in dissociation within the 2 ps simulation time, which agrees with the experimental finding that intact $[F{\cdot}H_2O]^+$ is not detected. All the other 39 singlet and 40 triplet trajectories resulted in prompt

dissociation into $H_2O^+$ + F. Analysis of the simulated trajectories indicates ultrafast dissociation of the H-F bond. The dissociation begins either at the instance of ionization or at a delay of 7-14 fs in which the H-F bond completes a half-oscillation. Surprisingly, the energetically favored $H_2F^+$ and $OH^+$ channels are not observed in the AIMD. Analysis of the ground state potential landscape shows that the path for forming $H_2F^+$ system must pass a transition state ~0.1eV above the $U_{FC}$, thus effectively blocking this channel on the ground state. In contrast, the pathway for $OH^+$ + HF formation exhibits a minimum at -2.9 eV, followed by a submerged barrier -1.1eV, i.e. below the $U_{FC}$. While the system certainly has enough energy to overcome this barrier, AIMD trajectories show that this is a narrow channel compared to the experimentally predominant path towards $H_2O^+$ + F.

The $OH^+$ + HF and $HF^+$ + OH channels could in principle be formed in a two-step process involving photodetachment first to the neutral potential followed by geometrical rearrangement and photoionization of either the OH or HF products. However, the observed $H_2F^+$ product is not likely to be formed on the neutral potential. In addition, previous intense field studies indicate that non-sequential double detachment is far more efficient than photodetachment, followed by photoionization.[13,19] Furthermore, high lying cation states were reported to form in intense field double detachment of tightly bound anionic molecular systems such as $SF_6^-$ and $F_2^-$.[18,19] Thus, the experimentally observed structural rearrangement to form $OH^+$ and $H_2F^+$ could in fact occur on excited cation states. Likewise, the formation of the observed $HF^+$ and $O^+$ products that cannot be reached energetically from the $U_{FC}$ cation ground state potential strongly suggests the contribution of excited cation states. Interestingly, although the relaxed energetic limits of the $F^+$ and $O^+$ cations are similar, only the later product is observed within experimental statistics.

In conclusion, we present a joint experimental-theoretical study of product formation on the $[F{\cdot}H_2O]^+$ surface produced by intense field double detachment of the $F^-{\cdot}H_2O$ anion. Unlike the previously explored dynamics on the neutral reactive surface leading to OH + HF,[32,35,38] $H_2O^+$ + F is the dominant experimental product. Although the relaxed limit of the $OH^+$ + HF is energetically favorable, AIMD trajectory simulations on both singlet and triplet ground states of $[F{\cdot}H_2O]^+$, initiated at the FC geometry of the anion, exhibit ultrafast dissociation of the H-F bond to form $H_2O^+$ + F. Similarly, although the surprising $H_2F^+$ + O channel is the most energetically favorable, it is not reproduced by the ground state AIMD trajectories, indicating significant barriers for the production of both $OH^+$ + HF and $H_2F^+$ + O. Thus, the observed formation of new bonds of the $H_2F^+$ cation is tentatively assigned to two roaming hydrogens dynamics on excited states of the $[F{\cdot}H_2O]^+$ complex. Excited state population in the intense field double detachment of the $F^-{\cdot}H_2O$ anion is further implied by the observed formation of the $O^+$ and $HF^+$ that are not energetically accessible from FC region of the cation ground state. Thus, intense-field multiple-electron detachment of anionic systems, which is intrinsically different from the ionization of neutral species, opens perspectives on new and very interesting chemical processes initiated at the stable anion geometry, including formation of new chemical bonds. Presenting challenges and opportunities for future studies including the theoretical description of minor products formation on excited cation states.

## Experimental and Theoretical methods

The experimental setup has been recently described in detail.[16–18,36] $F^-{\cdot}H_2O$ anions are prepared in an Even-Lavie cold ion source, accelerated and mass selected

before reaching a specially designed photofragment spectrometer.[36] In the photofragment spectrometer entrance, parent anions are further accelerated towards a field-free laser-anion interaction region. In the interaction region the ion beam is intersected by the optical path of a focused intense 800 nm laser. The ~35fs and ~3mJ pulses, allow reaching up to ~$3 \cdot 10^{15}$ W/cm$^2$ at the focal spot. The dependence of different processes on the laser peak intensity is examined by systematic displacement of the 250 mm focal length lens.[37]

While parent anions and anionic fragments are decelerated as they exit the spectrometer, neutral products retain their velocity and cations are accelerated. Thus, the TOF to a time and position sensitive coincidence imaging detector, distinguishes all possible photofragments based on their charge over mass ratios. The coincidence measurements are performed at low count rates, ensuring vanishing random coincidence and allowing construction of the coincidence map presented in figure 1.

AIMD simulations were performed on the lowest-lying singlet and triplet surfaces, using equation of motion coupled cluster theory with single and double excitations (EOM-CCSD) in the frozen core approximation.[41,42] This method was performed by double ionization of a well-behaved closed shell anionic reference state using the cc-pVTZ basis set.[41,42,45] This EOM-CCSD variant, provides a robust framework for treating the diradical character of the $[F \cdot H_2O]^+$ as well as the dissociation processes.[44,46,47]

40 initial geometries and velocities for both singlet and triplet AIMD simulations on the $[F \cdot H_2O]^+$ surface were sampled. This is expected to suffice for observing events with a statistical weight of a few percent. Initial conditions were sampled from four 250 fs AIMD trajectories of singlet $F^- \cdot H_2O$ using frozen core coupled cluster theory with single and double excitations (CCSD) and the cc-pVTZ basis

where each anion trajectory was initialized at the FC geometry with velocities sampled from a 300K Boltzmann distribution.[48] All trajectories were performed with 0.24 fs time steps.

Ground and excited state calculations along selected dissociation coordinates were performed at the frozen core equation of motion excitation energy coupled cluster theory with single, double, and perturbative triple excitations (EOM-CCSD(dT)) with the cc-pVTZ basis,[40,45,49–52] using a singlet restricted Hartree Fock reference of the anion.[40,53–55] Geometry optimizations and energy calculations of possible products and barriers were determined using the analogous coupled cluster theory with single, double and perturbative triple excitations (CCSD(T)) and the cc-pVTZ basis set.[56,57] All calculations shown were performed in the QChem electronic structure program package.[58]

## Acknowledgments

US-Israel BSF grant #2014701, Israel Science Foundation grant #1369/17, Zuckerman STEM Leadership Fellowship. The authors would also like to thank Professor Anna Krylov for her helpful comments on EOM methods.

**References**

(1) Posthumus, J. H. The Dynamics of Small Molecules in Intense Laser Fields. *Reports Prog. Phys.* **2004**, *67*, 623–665.
(2) Joachain, C. J.; Kylstra, N. J.; Potvliege, R. M. *Atoms in Intense Laser Fields*; 2012.
(3) Corkum, P. B. P. Plasma Perspective on Strong Field Multiphoton Ionization. *Phys. Rev. Lett.* **1993**, *71*, 1994–1997.
(4) Sheehy, B.; DiMauro, L. F. Atomic and Molecular Dynamics in Intense Optical Fields. *Annu. Rev. Phys. Chem.* **1996**, *47*, 463–494.
(5) Dörner, R.; Weber, T.; Weckenbrock, M.; Staudte, A.; Hattass, M.; Schmidt-Böcking, H.; Moshammer, R.; Ullrich, J. Multiple Ionization in Strong Laser Fields. In *Advances In Atomic, Molecular, and Optical Physics*; 2002; Vol. 48, pp 1–34.
(6) Corkum, P. B.; Krausz, F. Attosecond Science. *Nat. Phys.* **2007**, *3*, 381–387.
(7) Yamanouchi, K. Laser Chemistry and Physics: The Next Frontier. *Science (80-. ).* **2002**, *295*, 1659–1660.
(8) Ekanayake, N.; Nairat, M.; Kaderiya, B.; Feizollah, P.; Jochim, B.; Severt, T.; Berry, B.; Pandiri, K. R.; Carnes, K. D.; Pathak, S.; et al. Mechanisms and Time-Resolved Dynamics for Trihydrogen Cation ($H_3^+$) Formation from Organic Molecules in Strong Laser Fields. *Sci. Rep.* **2017**, *7*, 4703.

(9) Kiyan, I. Y.; Helm, H. Production of Energetic Electrons in the Process of Photodetachment of F-. *Phys. Rev. Lett.* **2003**, *90*, 183001.
(10) Pedregosa-Gutierrez, J.; Orr, P. A.; Greenwood, J. B.; Murphy, A.; Costello, J. T.; Zrost, K.; Ergler, T.; Moshammer, R.; Ullrich, J. Evidence for Rescattering in Intense, Femtosecond Laser Interactions with a Negative Ion. *Phys. Rev. Lett.* **2004**, *93*, 223001.
(11) Gazibegović-Busuladžić, A.; Milošević, D. B.; Becker, W.; Bergues, B.; Hultgren, H.; Kiyan, I. Y. Electron Rescattering in Above-Threshold Photodetachment of Negative Ions. *Phys. Rev. Lett.* **2010**, *104*, 103004.
(12) Hassouneh, O.; Law, S.; Shearer, S. F. C.; Brown, A. C.; van der Hart, H. W. Electron Rescattering in Strong-Field Photodetachment of $F^-$. *Phys. Rev. A* **2015**, *91*, 2–5.
(13) Albeck, Y.; Kandhasamy, D. M.; Strasser, D. Multiple Detachment of the $SF_6^-$ Molecular Anion with Shaped Intense Laser Pulses. *J. Phys. Chem. A* **2014**, *118*, 388–395.
(14) Bonacic-Koutecky, V.; Mitrić, R. Theoretical Exploration of Ultrafast Dynamics in Atomic Clusters: Analysis and Control. *Chem. Rev.* **2005**, *105*, 11–65.
(15) Wolf, S.; Sommerer, G.; Rutz, S.; Schreiber, E.; Leisner, T.; Wöste, L.; Berry, R. S. Spectroscopy of Size-Selected Neutral Clusters: Femtosecond Evolution of Neutral Silver Trimers. *Phys. Rev. Lett.* **1995**, *74*, 4177–4180.
(16) Albeck, Y.; Lerner, G.; Kandhasamy, D. M.; Chandrasekaran, V.; Strasser, D. Intense-Field Double Detachment of Electrostatically Bound $F^-(NF_3)_n$ Cluster Anions. *J. Phys. Chem. A* **2016**, *120*, 3246–3252.
(17) Albeck, Y.; Lerner, G.; Kandhasamy, D. M.; Chandrasekaran, V.; Strasser, D. Intense Field Double Detachment of Atomic versus Molecular Anions. *Phys. Rev. A* **2015**, *92*, 061401.
(18) Kandhasamy, D. M.; Albeck, Y.; Jagtap, K.; Strasser, D. 3D Coincidence Imaging Disentangles Intense Field Double Detachment of $SF_6^-$. *J. Phys. Chem. A* **2015**, *119*, 8076–8082.
(19) Shahi, A.; Albeck, Y.; Strasser, D. Intense-Field Multiple-Detachment of $F_2^-$: Competition with Photodissociation. *J. Phys. Chem. A* **2017**, *121*, 3037–3044.
(20) Muller, I. B.; Cederbaum, L. S. Microsolvation of $F^-$ in Water. *J. Phys. Chem. A* **2005**, *109*, 10424–10437.
(21) Townsend, D.; Lahankar, S. A.; Lee, S. K.; Chambreau, S. D.; Suits, A. G.; Zhang, X.; Rheinecker, J.; Harding, L. B.; Bowman, J. M. The Roaming Atom: Straying from the Reaction Path in Formaldehyde Decomposition. *Science (80-. ).* **2004**, *306*, 1158–1161.
(22) Mauguière, F. A. L.; Collins, P.; Stamatiadis, S.; Li, A.; Ezra, G. S.; Farantos, S. C.; Kramer, Z. C.; Carpenter, B. K.; Wiggins, S.; Guo, H. Toward Understanding the Roaming Mechanism in H + MgH → Mg + HH Reaction. *J. Phys. Chem. A* **2016**, *120*, 5145–5154.
(23) Joalland, B.; Shi, Y.; Kamasah, A.; Suits, A. G.; Mebel, A. M. Roaming Dynamics in Radical Addition-Elimination Reactions. *Nat. Commun.* **2014**, *5*, 1–6.
(24) Poisson, L.; Nandi, D.; Soep, B.; Hochlaf, M.; Boggio-Pasqua, M.; Mestdagh, J. M. A Roaming Wavepacket in the Dynamics of Electronically Excited 2-Hydroxypyridine. *Phys. Chem. Chem. Phys.* **2014**, *16*, 581–587.
(25) Bowman, J. M.; Houston, P. L. Theories and Simulations of Roaming. *Chem. Soc. Rev.* **2017**, *46*, 7615–7624.
(26) Robertson, W. H.; Johnson, M. A. Molecular Aspects of Halide Ion Hydration: The Cluster Approach. *Annu. Rev. Phys. Chem.* **2003**, *54*, 173–213.
(27) Mayhew, C. A.; Smith, D. The Reactions of F + Ions at Thermal Energies. *J. Phys. B At. Mol. Opt. Phys.* **1990**, *23*, 3139–3146.
(28) Luna, A.; Manuel, M.; Mo, O.; Yanez, M. G2 Ab Initio Calculations on the $F^+ + OH_2$ Singlet and Triplet Potential Energy Surfaces. *J. Phys. Chem.* **1994**, *98*, 6980–6987.
(29) Chaban, G. M.; Xantheas, S. S.; Gerber, R. B. Anharmonic Vibrational Spectroscopy of the $F^-(H_2O)_n$ Complexes,N= 1, 2. *J. Phys. Chem. A* **2003**, *107*, 4952–4956.
(30) Yang, X.; Wang, X.-B.; Wang, L.-S. Photodetachment of $F^-(H_2O)_n$ (N=1–4): Observation of Charge-Transfer States $[F^-(H_2O)_n^+]$ and the Transition State of $F+H_2O$ Hydrogen Abstraction Reaction. *J. Chem. Phys.* **2001**, *115*, 2889–2892.

(31) Ishikawa, Y.; Nakajima, T.; Yanai, T.; Hirao, K. Ab Initio Direct Molecular Dynamics Study of the Fragmentation of F($H_2O$) Complex Generated by Photodetachment of $F^-$($H_2O$) Anion Complex. *Chem. Phys. Lett.* **2002**, *363*, 458–464.
(32) Otto, R.; Ma, J.; Ray, A. W.; Daluz, J. S.; Li, J.; Guo, H.; Continetti, R. E. Imaging Dynamics on the F + $H_2O$ → HF + OH Potential Energy Surfaces from Wells to Barriers. *Science* **2014**, *343*, 396–399.
(33) Li, G.; Xie, Y.; Schaefer, H. F. From Gas-Phase to Liquid Water Chemical Reactions: The F + $(H_2O)_n$ , n = 1–4 Systems. *Chem. Phys. Lett.* **2016**, *648*, 1–7.
(34) Neumark, D. M. Probing the Transition State with Negative Ion Photodetachment: Experiment and Theory. *Phys. Chem. Chem. Phys* **2005**, *7*, 433–442.
(35) Ray, A. W.; Ma, J.; Otto, R.; Li, J.; Guo, H.; Continetti, R. E. Effects of Vibrational Excitation on the F + $H_2O$ → HF + OH Reaction: Dissociative Photodetachment of Overtone-Excited [F–H–OH] $^-$. *Chem. Sci.* **2017**, *8*, 7821–7833.
(36) Shahi, A.; Albeck, Y.; Strasser, D. Simultaneous 3D Coincidence Imaging of Cationic, Anionic, and Neutral Photo-Fragments. *Rev. Sci. Instrum.* **2018**, *89*, 013303.
(37) Albeck, Y.; Kandhasamy, D. M.; Strasser, D. Z-Scan Method for Nonlinear Saturation Intensity Determination, Using Focused Intense Laser Beams. *Phys. Rev. A* **2014**, *90*, 053422.
(38) Continetti, R. E.; Guo, H. Dynamics of Transient Species via Anion Photodetachment. *Chem. Soc. Rev.* **2017**, *46*, 7650–7667.
(39) Zhao, B.; Guo, H. Modulations of Transition-State Control of State-to-State Dynamics in the F + H 2 O → HF + OH Reaction. *J. Phys. Chem. Lett.* **2015**, *6*, 676–680.
(40) Stanton, J. F.; Bartlett, R. J. The Equation of Motion Coupled-Cluster Method. A Systematic Biorthogonal Approach to Molecular Excitation Energies, Transition Probabilities, and Excited State Properties. *J. Chem. Phys.* **1993**, *98*, 7029–7039.
(41) Kuś, T.; Krylov, A. I. Using the Charge-Stabilization Technique in the Double Ionization Potential Equation-of-Motion Calculations with Dianion References. *J. Chem. Phys.* **2011**, *135*, 084109.
(42) Kuś, T.; Krylov, A. I. De-Perturbative Corrections for Charge-Stabilized Double Ionization Potential Equation-of-Motion Coupled-Cluster Method. *J. Chem. Phys.* **2012**, *136*, 244109.
(43) Kállay, M.; Gauss, J. Calculation of Excited-State Properties Using General Coupled-Cluster and Configuration-Interaction Models. *J. Chem. Phys.* **2004**, *121*, 9257–9269.
(44) Krylov, A. I. Equation-of-Motion Coupled-Cluster Methods for Open-Shell and Electronically Excited Species: The Hitchhiker's Guide to Fock Space. *Annu. Rev. Phys. Chem.* **2008**, *59*, 433–462.
(45) Dunning, T. H. Gaussian Basis Sets for Use in Correlated Molecular Calculations. I. The Atoms Boron through Neon and Hydrogen. *J. Chem. Phys.* **1989**, *90*, 1007–1023.
(46) Nooijen, M. State Selective Equation of Motion Coupled Cluster Theory: Some Preliminary Results. *Int. J. Mol. Sci.* **2002**, *3*, 656–675.
(47) Sattelmeyer, K. W.; Schaefer III, H. F.; Stanton, J. F. Use of 2h and 3h−p-like Coupled-Cluster Tamm–Dancoff Approaches for the Equilibrium Properties of Ozone. *Chem. Phys. Lett.* **2003**, *378*, 42–46.
(48) Purvis, G. D.; Bartlett, R. J. A Full Coupled-Cluster Singles and Doubles Model: The Inclusion of Disconnected Triples. *J. Chem. Phys.* **1982**, *76*, 1910–1918.
(49) Krylov, A. I.; Sherrill, C. D.; Head-Gordon, M. Excited States Theory for Optimized Orbitals and Valence Optimized Orbitals Coupled-Cluster Doubles Models. *J. Chem. Phys.* **2000**, *113*, 6509–6527.
(50) Sekino, H.; Bartlett, R. J. A Linear Response, Coupled-cluster Theory for Excitation Energy. *Int. J. Quantum Chem.* **1984**, *26*, 255–265.
(51) Koch, H.; Jensen, H. J. A.; Joergensen, P.; Helgaker, T. Excitation Energies from the Coupled Cluster Singles and Doubles Linear Response Function (CCSDLR). Applications to Be, $CH^+$ , CO, and $H_2O$. *J. Chem. Phys.* **1990**, *93*, 3345–3350.
(52) Manohar, P. U.; Krylov, A. I. A Noniterative Perturbative Triples Correction for the Spin-Flipping and Spin-Conserving Equation-of-Motion Coupled-Cluster Methods with Single and Double Substitutions. *J. Chem. Phys.* **2008**, *129*, 194105.

(53) Hartree, D. R. The Wave Mechanics of an Atom with a Non-Coulomb Central Field. Part I. Theory and Methods. *Math. Proc. Cambridge Philos. Soc.* **1928**, *24*, 89.
(54) Fock, V. Näherungsmethode Zur Losung Des Quantenmechanischen Mehrkorperproblems. *Zeitschrift fur Phys.* **1930**, *61*, 126–148.
(55) Piecuch, P.; Włoch, M. Renormalized Coupled-Cluster Methods Exploiting Left Eigenstates of the Similarity-Transformed Hamiltonian. *J. Chem. Phys.* **2005**, *123*, 224105.
(56) Raghavachari, K.; Trucks, G. W.; Pople, J. A.; Head-Gordon, M. A Fifth-Order Perturbation Comparison of Electron Correlation Theories. *Chem. Phys. Lett.* **1989**, *157*, 479–483.
(57) Bartlett, R. J.; Watts, J. D.; Kucharski, S. A.; Noga, J. Non-Iterative Fifth-Order Triple and Quadruple Excitation Energy Corrections in Correlated Methods. *Chem. Phys. Lett.* **1990**, *165*, 513–522.
(58) Shao, Y.; Gan, Z.; Epifanovsky, E.; Gilbert, A. T. B.; Wormit, M.; Kussmann, J.; Lange, A. W.; Behn, A.; Deng, J.; Feng, X.; et al. Advances in Molecular Quantum Chemistry Contained in the Q-Chem 4 Program Package. *Mol. Phys.* **2015**, *113*, 184–215.